

Contribution from Lash Miller Chemical Laboratories and Erindale College,
University of Toronto, Toronto, Ontario, Canada M5S 1A1**Cobalt Atom–Carbon Monoxide–Dioxygen Cryochemistry: Infrared and Ultraviolet–Visible Spectroscopic Studies of $\text{Co}(\text{CO})_n(\text{O}_2)$ (Where $n = 1-4$)**

GEOFFREY A. OZIN,* A. J. LEE HANLAN, and WILLIAM J. POWER

Received October 13, 1978

Cocondensation reactions of Co atoms with CO/O_2 mixtures at 10–12 K give rise to a plethora of reaction products, the number and distribution of which are highly sensitive to the cobalt concentration, the CO/O_2 ratio, and the presence or absence of an inert diluent such as Ar. When conditions are chosen so as to promote mononuclear reaction products, one can identify by IR spectroscopy, besides $\text{Co}(\text{CO})_n$ (where $n = 4-1$) and $\text{Co}(\text{O}_2)_m$ (where $m = 2, 1$) parents, at least four mixed carbonyl–dioxygen complexes of the form $\text{Co}(\text{CO})_n(\text{O}_2)$ absorbing in the 2100–2000- cm^{-1} $\nu(\text{CO})$ region and the 1130–1120/970–940- cm^{-1} $\nu(\text{OO})$ region. Concentration, warm-up, and $^{12}\text{C}^{16}\text{O}/^{16}\text{O}_2/^{18}\text{O}_2$ and $^{12}\text{C}^{16}\text{O}/^{16}\text{O}_2/^{16}\text{O}^{18}\text{O}/^{18}\text{O}_2$ isotopic substitution experiments point favorably toward a mono(dioxygen) formulation for the complete series $\text{Co}(\text{CO})_n(\text{O}_2)$ (where $n = 1-4$) of complexes. Significantly, when $n = 1-3$, the dioxygen moiety absorbs in the low-frequency $\nu(\text{OO})$ range (970–940 cm^{-1}), close to that of the $\text{Co}(\text{O}_2)$ parent at 954 cm^{-1} (cf. $\text{Ni}(\text{O}_2)$ at 966 cm^{-1} and $\text{Cu}(\text{O}_2)$ at 1016 cm^{-1}), and is tentatively associated with side-on dioxygen coordination. Only when $n = 4$ does the $\nu(\text{OO})$ mode blue-shift into the high-frequency range (1124 cm^{-1}), close to that of free superoxide (1097 cm^{-1}), suggesting a molecular ion-pair $[\text{Co}(\text{CO})_4]^+\text{O}_2^-$ formulation for the highest stoichiometry complex in the system. This proposal can be considered to be in line with recent ESR detection of $\text{Co}(\text{CO})_4(\text{O}_2)$, purported to be the condensation product of $\text{Co}(\text{CO})_4$ (from gas-phase thermal dissociation of $\text{Co}_2(\text{CO})_8$) and O_2 onto a 77 K cold finger. The corresponding optical data for $\text{Co}(\text{CO})_4(\text{O}_2)$ are interpreted in terms of a pseudotetrahedral d^8 tetracarbonylcobalt(I)–superoxide ion pair (the cationic moiety being related to its isoelectronic d^8 (C_{2v}) neighbor $\text{Fe}(\text{CO})_4$) with $\text{Co}(d) \rightarrow \text{CO}(\pi^*)$ MLCT transitions in the range 220–230 nm and $\text{CO}(\sigma) \rightarrow \text{Co}(d)$ LMCT transitions around 370 nm, having undergone the anticipated *blue* and *red* shifts, respectively, from the related MLCT/LMCT excitations of the d^9 tetracarbonylcobalt(0) radical species (the latter occurring in the ranges 245–257 and 310–358 nm, respectively).

Introduction

Not a great deal is presently recorded about the matrix chemistry of cobalt vapor. It is known that cobalt atom aggregation is an extremely facile process in Ar, Kr, Xe, and CH_4 matrices deposited at 12–20 K, as seen from the recent optical spectroscopic detection of Co_2 , Co_3 , and higher Co_n clusters.¹ Such reactions in the presence of CO have been shown by IR, Raman, UV–vis, and ESR spectroscopies to give birth to $\text{Co}(\text{CO})_n$ and $\text{Co}_2(\text{CO})_m$ (where $n = 1-4$ and $m \leq 8$).² Similar reactions with N_2 also lead to a profusion of $\text{Co}(\text{N}_2)_n/\text{Co}_2(\text{N}_2)_m$ products, although the values of n and m have yet to be established.³ Cobalt–dioxygen cocondensations,⁴ like rhodium–dioxygen matrix processes,⁵ also yield a number of mononuclear and higher cluster complexes; however, in the case of cobalt atoms, only $\text{Co}(\text{O}_2)_n$ (where $n = 1, 2$) are reasonably well characterized. A recent study involving cobalt–ethylene matrix cocondensations clearly demonstrated the existence of $\text{Co}(\text{C}_2\text{H}_4)_n/\text{Co}_2(\text{C}_2\text{H}_4)_m$ (where $n = 1, 2$) as well as a possible tetranuclear product $\text{Co}_4(\text{C}_2\text{H}_4)_m$ (where m is probably 1 or 4).⁶

In the majority of the matrix studies of cobalt vapor, careful concentration experiments involving metal and ligand, together with ligand isotope substitution investigations, were needed to establish metal nuclearity and ligand stoichiometry.¹⁻⁶ Aside from the macroscale synthetic chemistry of cobalt vapor involving multiple-ligand mixtures,⁷ no comparable matrix reaction chemistry of cobalt vapor has been reported. As a move in this direction we have now investigated the cobalt–carbon monoxide–dioxygen system. This was in part motivated by our earlier investigations of $\text{M}/\text{CO}/\text{O}_2$ ^{8,9} and $\text{M}/\text{C}_2\text{H}_4/\text{O}_2$ ¹⁰ reactions with the group 1B metal atoms (Ag, Au) and $\text{M}/\text{CO}/\text{N}_2$ ¹¹ and $\text{M}/\text{O}_2/\text{N}_2$ ¹² reactions involving the group 8 metal atoms (Ni, Pd, Pt). In the case of silver, $[(\text{OC})\text{Ag}]^+\text{O}_2^-$, a thermally labile superoxide complex, was the sole product,⁸ whereas in the case of gold

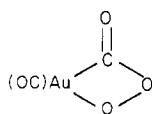
a peroxyformate reaction product could be generated which, on thermalizing at 30–40 K, fragmented to CO_2 and gold clusters.⁹ The cobalt system was expected to be somewhat different from those of silver and gold in view of the ease of generating $\text{Co}(\text{CO})_n$ (where $n = 1-4$)² and the recent report that $\text{Co}(\text{CO})_4$ (present in small quantities in the vapor of $\text{Co}_2(\text{CO})_8$) reacts with O_2 at 77 K to form $\text{Co}(\text{CO})_4(\text{O}_2)$. The latter complex, detected by Symons et al.¹³ by ESR spectroscopy, has a considerably reduced hyperfine coupling to ^{59}Co compared to that found in $\text{Co}(\text{CO})_4$.^{2,13} The unpaired electron in $\text{Co}(\text{CO})_4(\text{O}_2)$ was concluded to be strongly confined to the two oxygen atoms.¹³ Approximate 4s and 3d_{z²} hyperfine tensor components were computed at only 1.0 and 1.4%, respectively. A superoxide formulation of the type $[\text{Co}(\text{CO})_4]^+\text{O}_2^-$ would therefore not be unreasonable for $\text{Co}(\text{CO})_4(\text{O}_2)$ where the 16-electron $[\text{Co}(\text{CO})_4]^+$ cation is of interest from the point of view of its molecular and electronic properties with respect to its d^8 isoelectronic neighbor $\text{Fe}(\text{CO})_4$.¹⁴

In what follows we will present the IR and UV–vis spectroscopic evidence for $\text{Co}/\text{O}_2/\text{CO}$ matrix reaction products which points to the existence of a complete series of mixed dioxygen–carbonyl mononuclear complexes of the type $\text{Co}(\text{CO})_n(\text{O}_2)$.

Experimental Section

Monoatomic Co vapor was generated by directly heating a 0.010 in. ribbon filament of the metal with ac in a furnace which has been described previously.¹⁵ The cobalt metal (99.99%) was supplied by McKay Inc., New York. Research grade $^{16}\text{O}_2$ (99.99%), $^{12}\text{C}^{16}\text{O}$ (99.99%), and Ar (99.99%) were supplied by Matheson. Isotopically enriched $^{18}\text{O}_2$ (93%) was supplied by Miles Research Laboratories. Statistically scrambled mixtures of $^{16}\text{O}_2/^{16}\text{O}^{18}\text{O}/^{18}\text{O}_2$ were prepared by subjecting $^{16}\text{O}_2/^{18}\text{O}_2$ mixtures at about 200 torr to a continuous tesla discharge.

The rate of metal atom deposition was continuously monitored and controlled by using a quartz crystal microbalance.¹⁶ The deposition rate was set such that the probability of a metal atom having another metal atom as nearest neighbor in the matrix was approximately 1/1000. Matrix gas flows, controlled by a calibrated micrometer needle valve, were maintained in the range 1–2 mmol/h. In the infrared experiments the matrices were deposited on a CsI window cooled to 10–12 K by means of an Air Products Displex closed-cycle



helium refrigerator. IR spectra were recorded with a Perkin-Elmer 180 spectrophotometer. In the UV-visible experiments, the matrices were deposited on a NaCl window with the spectra recorded on a Varian Techtron spectrophotometer.

Results and Discussion

Infrared Experiments. Cobalt atom matrix reactions have to be treated with caution because of the propensity toward small-cluster complex formation.¹ In this particular study, aggregation was deliberately minimized by operating in the mononuclear regime of less than 0.01% cobalt. The pure Co/CO system is considered to be thoroughly understood under high-dispersion conditions, where four paramagnetic binary carbonyl $\text{Co}(\text{CO})_n$ species ($n = 1-4$) have been identified and their structures defined as linear, linear, C_{3v} pyramidal, and C_{3v} distorted tetrahedral, respectively.² Their $\nu(\text{CO})$ stretching (in solid Ar) modes are as follows: $\text{Co}(\text{CO})$, 1956/1949; $\text{Co}(\text{CO})_2$, 1919; $\text{Co}(\text{CO})_3$, 1982; $\text{Co}(\text{CO})_4$, 2024/2014 cm^{-1} . Less well understood at this time is the Co/O₂ system.⁴ Although mononuclear $\text{Co}(\text{O}_2)_n$ (where $n = 1, 2$) dioxygen complexes, by analogy with $\text{Ni}(\text{O}_2)_n$ and $\text{Cu}(\text{O}_2)_n$ complexes, are not unexpected products (see trend in $\nu(\text{OO})$ stretching frequencies expected with increasing effective nuclear charge on the metal)

| complex | $\nu(\text{OO}), \text{cm}^{-1}$ | | |
|---------------------------------|----------------------------------|----------------------|----------------------|
| | M = Co ⁴ | M = Ni ¹⁷ | M = Cu ¹⁸ |
| M(O ₂) | 954 | 966 | 1016 |
| M(O ₂) ₂ | 1026 | 1062 | 1112 |

the binuclear and higher $\text{Co}_m(\text{O}_2)_n$ cluster products that clearly exist in the system at low cobalt dispersions have yet to be clarified.⁴

In an attempt to define the number and nature of the cobalt-dioxygen-carbonyl reaction products formed at 10–12 K, a large number of Co atom condensations with CO/O₂ and CO/O₂/Ar mixtures have been conducted. Our strategy basically involved an IR (and UV-vis whenever experimentally feasible) spectroscopic examination of product distributions in CO/O₂ \approx 1/1, 1/4 and 4/1 and CO/O₂/Ar \approx 1/1/10, 1/4/10, 4/1/10, 1/1/50, 4/1/50, and 1/4/50 matrix condensations. Of greatest value in these analyses were the $\nu(\text{CO})$ and $\nu(\text{OO})$ fingerprint vibrations coupled with confirmatory ¹⁶O₂/¹⁸O₂ and ¹⁶O₂/¹⁶O¹⁸O/¹⁸O₂ isotopic substitution experiments. Band overlap in the $\nu(\text{CO})$ region unfortunately precluded any definitive ¹²C¹⁶O/¹³C¹⁶O isotopic pinpointing of CO stoichiometry from the carbonyl portion of the spectra.

Let us consider first some representative IR results obtained under dilute CO/O₂/Ar \approx 1/1/50 conditions. A typical spectrum in the carbonyl region is illustrated in Figure 1 for a 10–12 K deposition. Easily discernible among the profusion of lines are those associated with $\text{Co}(\text{CO})$ (1956), $\text{Co}(\text{CO})_2$ (1919), $\text{Co}(\text{CO})_3$ (1982), and $\text{Co}(\text{CO})_4$ (2014 cm^{-1}). Care must be exercised not to confuse the natural-abundance ¹³C¹⁶O/¹²C¹⁸O isotopic components (around 2090 cm^{-1}) of ¹²C¹⁶O with a product absorption, especially as close coincidences in this region turn out to be of central importance in the assignments to be expounded. The most striking new spectral features noticed on deposition under 1/1/50 reaction conditions can be seen in Figure 1 to occur at 2069 (I), 2020 (II), and 2076/2046 (III) cm^{-1} . Warm-up experiments in the 10–40 K temperature range necessitate that these new absorptions be assigned to *three* independent complexes with associated $\nu(\text{OO})$ stretching modes (roughly one to two orders of magnitude less intense than the corresponding $\nu(\text{CO})$ absorptions) at roughly 970 (I), 950 (II), and 940 (III) cm^{-1} , respectively.¹⁹ The course and outcome of a series of warm-up experiments are laid out in Figure 1B–D from which it can be determined that species labeled I and II gradually decay to zero (together with $\text{Co}(\text{CO})$, $\text{Co}(\text{CO})_2$, and $\text{Co}(\text{CO})_3$) with

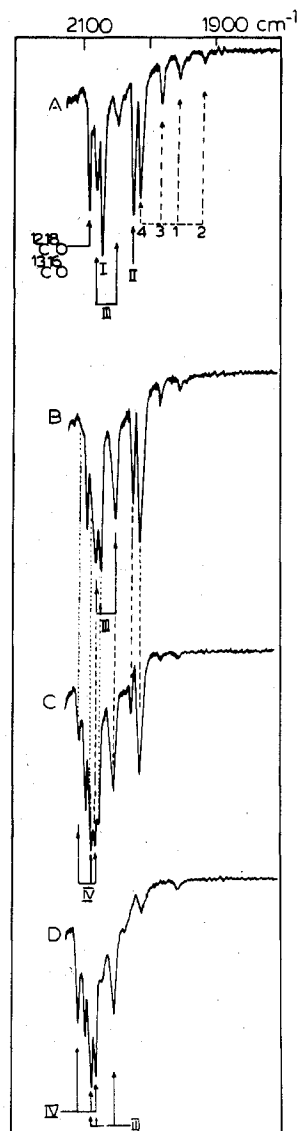


Figure 1. Matrix infrared spectrum of the products formed on depositing Co atoms with CO/O₂/Ar \approx 1/1/50 mixtures: (A) at 10–12 K showing $\text{Co}(\text{CO})_{1-4}$ (labeled 1, 2, 3, 4) co-isolated with mixed dioxygen-carbonyl complexes $\text{Co}(\text{CO})_n(\text{O}_2)$ labeled I, II, and III; B–D show the progress of 20, 30, and 35 K annealing experiments in which the appearance of IV is revealed. In all figures I \equiv $\text{Co}(\text{CO})(\text{O}_2)$, II \equiv $\text{Co}(\text{CO})_2(\text{O}_2)$, III \equiv $\text{Co}(\text{CO})_3(\text{O}_2)$, and IV \equiv $\text{Co}(\text{CO})_4(\text{O}_2)$.

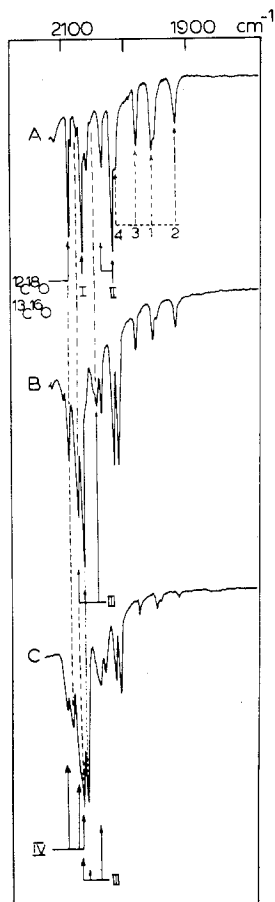
concomitant growth of lines associated with III and appearance of a *fourth* new species absorbing at 2102, 2082, and 2076 cm^{-1} (labeled IV) in the $\nu(\text{CO})$ region and around 1124 cm^{-1} in the $\nu(\text{OO})$ region. Warming into the 30–35 K range shows gradual decay of the bands connected with III, leaving behind those ascribed to IV. Although frustrated by ¹²C¹⁶O/¹³C¹⁶O isotopic-overlap problems in the $\nu(\text{CO})$ region and ¹⁶O₂/¹⁸O₂ and ¹⁶O₂/¹⁶O¹⁸O/¹⁸O₂ intensity complications in the $\nu(\text{OO})$ region, it was nevertheless possible to establish the dioxygen stoichiometry to be unity (i.e., observation of simple 59–66- cm^{-1} ¹⁶O₂/¹⁸O₂ isotopic doublets)¹⁷ for all four carbonyl-dioxygen complexes I–IV as shown in Table I.

The only effect of diluting the matrix mixture further with dioxygen (for example, by using CO/O₂/Ar \approx 1/4/50) was to emphasize the isolation of the presumed lower CO stoichiometry complexes I (2069/2062 cm^{-1}) and II (2020/2038 cm^{-1}) (pronounced multiple trapping site effects seem to be encouraged by dilution) with the noticeable absence of III and IV (see Figure 2A); note also the absence of $\text{Co}(\text{CO})_4$ and the intensity ordering $\text{Co}(\text{CO}) > \text{Co}(\text{CO})_2 \approx \text{Co}(\text{CO})_3$ on de-

Table I. Infrared Dioxygen Isotopic Substitution Data for $\text{Co}(\text{CO})_n(\text{O}_2)$ (Where $n = 1-4$)

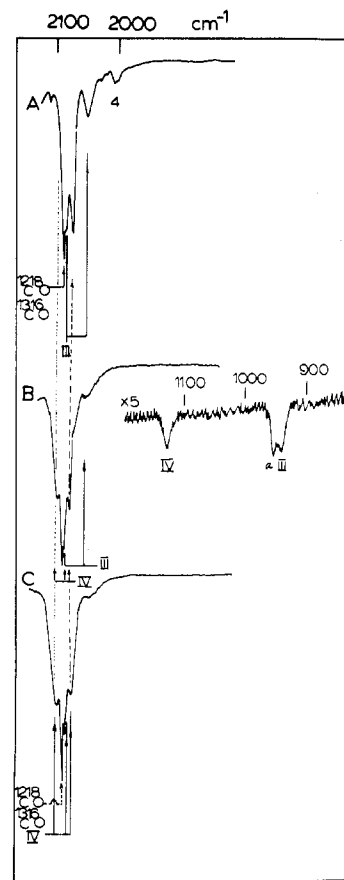
| | $\nu(^{16}\text{O}^{16}\text{O})$ | $\nu(^{18}\text{O}^{18}\text{O})$ | $\nu(^{16}\text{O}^{18}\text{O})$ | $\Delta\nu(^{16}\text{O}_2-^{18}\text{O}_2)$ |
|-----|-----------------------------------|-----------------------------------|-----------------------------------|--|
| I | 972 | 910 | <i>b</i> | 62 |
| II | 950 | 891 | 920 ^a | 59 |
| III | 940 | 878 | | 62 |
| IV | 1124 | 1058 | 1094 | 66 |

^a Broad line probably due to overlap between $^{16}\text{O}^{18}\text{O}$ stretching modes of II and III. ^b Not observed through band-overlap complications with II and III. The $^{16}\text{O}^{18}\text{O}$ absorptions were too broad and weak to stand any chance of permitting differentiation between end-on and side-on modes of dioxygen coordination.^{17,18}

**Figure 2.** (A) The same as Figure 1 except a $\text{CO}/\text{O}_2/\text{Ar} \approx 1/4/50$ mixture was employed with annealing at (B) 20 K and (C) 30 K.

position. As expected, warming to 20–30 K (Figure 2B,C) encourages rapid growth of $\text{Co}(\text{CO})_4$ and decay of $\text{Co}(\text{CO})_{1,2,3}$ with concurrent appearance of III followed by some IV and loss of I and II. These observations lend considerable strength to the assignment of *four* new species $\text{Co}(\text{CO})_n(\text{O}_2)$ coexisting with the four parent carbonyls $\text{Co}(\text{CO})_n$ (where $n = 1-4$).

IR experiments performed in pure CO/O_2 mixtures, ranging in value from 4/1 to 1/1 to 1/4, spelled out roughly the same scenario as that experienced in argon-diluted experiments, except that the highest stoichiometry species III and IV dominated the spectra. For instance, in $\text{CO}/\text{O}_2 \approx 1/4$ depositions at 10–12 K (Figure 3A) besides a trace of $\text{Co}(\text{CO})_4$ one observes the $\nu(\text{CO})$ modes of III at 2086, 2076, and 2050 cm^{-1} with $\nu(\text{OO})$ at 944 cm^{-1} in the presence of traces of IV. Warming to 25–30 K causes substantial conversion to complex IV (Figure 3B,C), as seen by gradual collapse of the $\nu(\text{CO})$ and $\nu(\text{OO})$ modes of III and concomitant growth of the $\nu(\text{CO})$ and $\nu(\text{OO})$ modes of IV at 2100, 2084, and 2075 cm^{-1} and 1124 cm^{-1} , respectively. Experiments of this type alert one

**Figure 3.** (A) The same as Figure 1 except a $\text{CO}/\text{O}_2 \approx 1/4$ mixture was employed with annealing at (B) 25 K and (C) 35 K. “a” represents the $\nu(\text{OO})$ mode of $\text{Co}(\text{O}_2)$.

to the overlap complications that exist between the $\nu(\text{CO})$ modes of III and IV in the 2100–2070- cm^{-1} region.

Depositions richer in CO, for example, $\text{CO}/\text{O}_2 \approx 4/1$, yield a product distribution dominated by $\text{Co}(\text{CO})_4$ with both III and IV co-isolated at 10–12 K. Other than a greater opportunity for the $2\text{Co}(\text{CO})_4 \rightarrow \text{Co}_2(\text{CO})_8$ competing matrix dimerization process, evidence for which can be secured by scanning the 1860–1840- cm^{-1} $\nu(\text{CO})$ bridge region of $\text{Co}_2(\text{CO})_8$ and was most apparent in $\text{CO}/\text{O}_2 \approx 4/1$ mixtures,²⁰ the spectra of III and IV were essentially the same as in Ar- and O_2 -rich matrices, and the preponderance of IV at 35 K was again evident. Finally, roughly equimolar ($\text{CO}/\text{O}_2 \approx 1/1$) depositions at 10–12 K (Figure 4A) yielded a product distribution comprising mainly species III with smaller amounts of II and $\text{Co}(\text{CO})_4$. Warming in the range 20–30 K causes collapse of the $\text{Co}(\text{CO})_4$ and II peaks simultaneously with the growth of IV and slight decay of III (Figure 4B–D). Again, subtle band shifting and intensity alterations in the 2100–2070- cm^{-1} region point out the overlap phenomenon between $\nu(\text{CO})$ bands of III and IV but nevertheless generally concur with the observations in dilute matrices and lead to a consistent set of assignments for $\text{Co}(\text{CO})_n(\text{O}_2)$ (where $n = 1-4$), as listed in Table II.

A final point regarding metal–ligand stretching and deformational modes should be mentioned. Spectral scanning of the low-frequency region throughout the aforementioned IR experiments consistently revealed a number of absorptions in the 500–300- cm^{-1} region that could be associated with the proposed $\text{Co}(\text{CO})_n(\text{O}_2)$ complexes. Assignment of lines to specific species in dilute $\text{CO}/\text{O}_2/\text{Ar}$ mixtures was complicated for reasons similar to those delineated for the $\nu(\text{CO})$ modes. However, in pure CO/O_2 mixtures it was possible to associate three new lines at 466, 397, and 384 cm^{-1} with species IV and

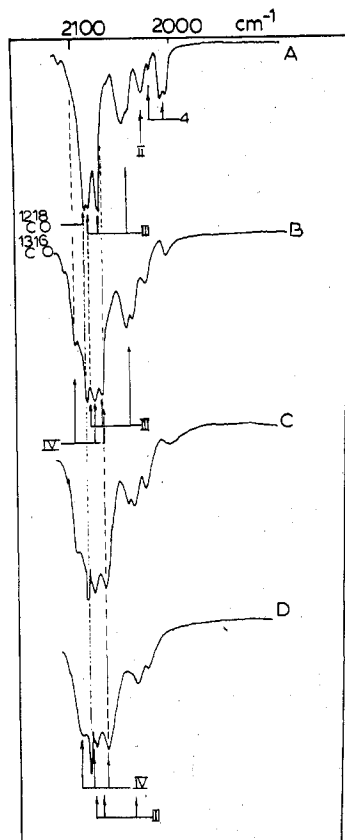


Figure 4. (A) The same as Figure 1 except a $\text{CO}/\text{O}_2 \approx 1/1$ mixture was employed with annealing at (B) 25 K, (C) 30 K, and (D) 35 K.

Table II. Assignments of the Major $\nu(\text{CO})$ and $\nu(\text{OO})$ Absorptions Ascribed to $\text{Co}(\text{CO})_n(\text{O}_2)$ (Where $n = 1-4$)

| label | complex | $\nu(\text{CO})^a$ | $\nu(\text{OO})$ |
|-------|--------------------------------------|-------------------------------------|------------------|
| I | $\text{Co}(\text{CO})(\text{O}_2)$ | 2069 ⁱ | 970 |
| II | $\text{Co}(\text{CO})_2(\text{O}_2)$ | 2020 ⁱⁱ | 950 |
| III | $\text{Co}(\text{CO})_3(\text{O}_2)$ | 2086 2076 2046 ⁱⁱⁱ | 940 |
| IV | $\text{Co}(\text{CO})_4(\text{O}_2)$ | 2102 2082 2076 | 1124 |

^a Depending on matrix deposition and concentration conditions these bands are subject to matrix site or multiple trapping site splittings: i, 2069/2062 cm^{-1} ; ii, 2035/2020 cm^{-1} ; iii, 2050/2046 cm^{-1} . These effects are less noticeable in CO/O_2 matrices than dilute $\text{CO}/\text{O}_2/\text{Ar}$ matrices.

two new lines at 478 and 438 cm^{-1} possibly with species III in the presence of the most intense $\nu(\text{CoC})$ stretching mode of $\text{Co}(\text{CO})_4^2$ at 486 cm^{-1} . These vibrational modes are likely to be associated with $\nu(\text{CoC})$, $\delta(\text{CoCO})$, and $\nu(\text{CoO})$ motions.^{2,5,17} However, with the available data a more definite assignment is not possible at this time.

Ultraviolet-Visible Experiments. In order to obviate spectral ambiguities originating from band-overlap complications between $\text{Co}(\text{CO})_n$ and $\text{Co}(\text{CO})_n(\text{O}_2)$ absorptions as well as with Co atomic resonance lines¹ (most pronounced in dilute $\text{CO}/\text{O}_2/\text{Ar}$ mixtures), one is obliged to operate in pure CO/O_2 mixtures ranging from 1/4 to 4/1. Under these conditions the corresponding IR spectra show the presence of varying proportions of $\text{Co}(\text{CO})_4$, $\text{Co}(\text{CO})_4(\text{O}_2)$, and $\text{Co}(\text{CO})_3(\text{O}_2)$ as the major absorbing species. The discussion to follow will therefore focus its attention on the optical spectroscopy of $\text{Co}/\text{CO}/\text{O}_2$ cocondensations.

With prior knowledge of the optical spectra and band assignments of $\text{Co}(\text{CO})_4$ at hand (see ref 1, Figure 5, and

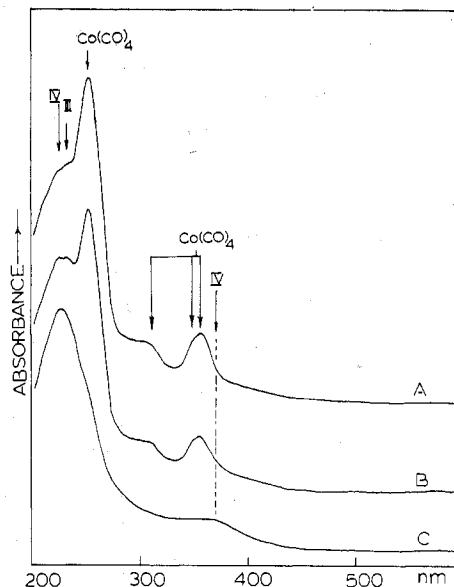


Figure 5. UV-visible spectra of the products formed on cocondensing cobalt atoms with $\text{CO}/\text{O}_2 \approx 1/1$ mixtures (A) after deposition at 10–12 K; B and C show the progress of 20–25 and 30–35 K warm-up experiments.

Table IV), one can easily pinpoint electronic transitions of product $\text{Co}(\text{CO})_4$ in $\text{CO}/\text{O}_2 \approx 1/1$ mixtures at 10–12 K (Figure 5A). The associated IR spectroscopy of such matrices depicts the presence of major concentrations of III co-isolated with $\text{Co}(\text{CO})_4$ and trace amounts of II. However, brief warming to 25 K is sufficient to induce substantial loss of $\text{Co}(\text{CO})_4$ and II with concomitant appearance of IV. This behavior is reflected optically in Figure 5A–C where on deposition a new broad feature can be seen as a high-energy shoulder on the 252-nm $\text{Co}(\text{d}) \rightarrow \text{CO}(\pi^*)$ MLCT band of $\text{Co}(\text{CO})_4$. At this stage one is obliged to connect the 225–235-nm absorption mainly with compound III. Warming to 20–25 K causes gradual collapse of both $\text{Co}(\text{CO})_4$ MLCT and LMCT absorptions (Figure 5B) to the point of disappearance at 30–35 K (Figure 5C). At this point of product development, the optical spectrum that emerges is quite distinct from that of $\text{Co}(\text{CO})_4$, showing absorption maxima at 226 and 367 nm, the high-energy band being by far the more intense. The annealing behavior of these two new bands points to a single absorbing species and hence an association with $\text{Co}(\text{CO})_4(\text{O}_2)$ (IV). One must presume that any related MLCT bands tied in with $\text{Co}(\text{CO})_3(\text{O}_2)$ (III) are overlapped with and remain hidden by the intense MLCT absorptions of $\text{Co}(\text{CO})_4$ and $\text{Co}(\text{CO})_4(\text{O}_2)$ throughout the deposition and warm-up events illustrated in Figure 5.

Following the leads of the IR experiments which point to a predominance of species III with some $\text{Co}(\text{CO})_4$ on depositing Co atoms with oxygen-rich matrices ($\text{CO}/\text{O}_2 \approx 1/4$), one notices in the corresponding optical spectra (Figure 6A) a diminished importance of the $\text{Co}(\text{CO})_4$ MLCT absorption centered around 245 nm (in these matrices) with respect to the high-energy shoulder which now displays resolved doublet structure at 222 and 232 nm (Table IV). According to the IR observations, warming these matrices to 20–30 K causes rapid consumption of $\text{Co}(\text{CO})_4$ with concurrent growth of IV. These effects are manifested in the optical spectrum (Figure 6B,C) by the loss of $\text{Co}(\text{CO})_4$ bands around 245, 310, 350, and 358 nm and with the growth of the broad 222–232-nm feature in unison with a weak band around 370 nm, a sequence of events reminiscent of those recorded in $\text{CO}/\text{O}_2 \approx 1/1$ mixtures. Clearly with the available data it is quite difficult to unequivocally associate optical absorptions with III and IV. Similar experiments performed in $\text{CO}/\text{O}_2 \approx 4/1$ mixtures,

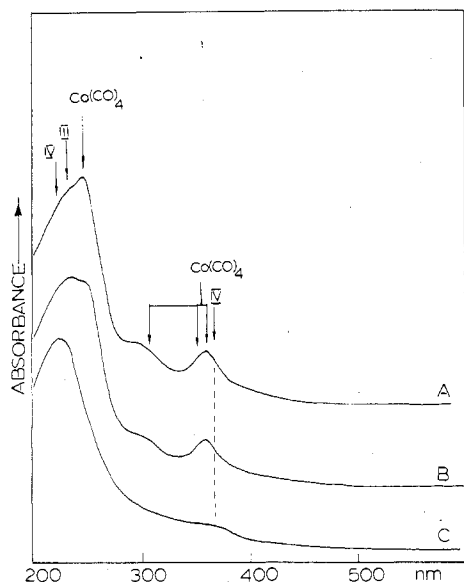


Figure 6. The same as Figure 5 except that $\text{CO}/\text{O}_2 \approx 1/4$ mixtures were used.

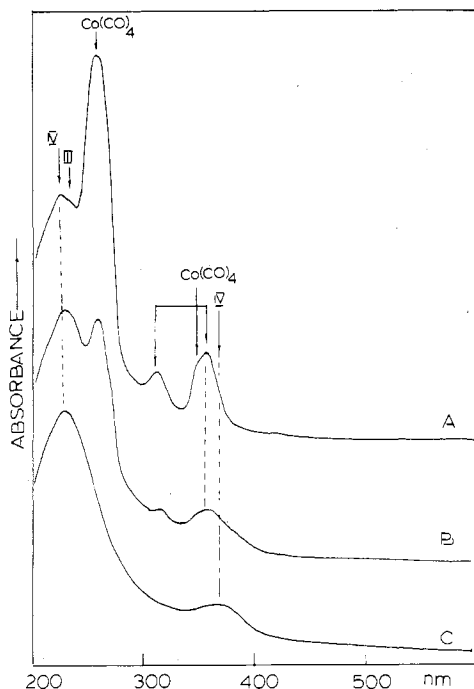


Figure 7. The same as Figure 5 except $\text{CO}/\text{O}_2 \approx 4/1$ mixtures were used.

although spectroscopically pleasing (Figure 7), did not really assist one any further in the clarification of the optical assignments of species III and IV. All that one can say is that both III and IV exhibit MLCT transitions in the region of 220–230 nm, having undergone a *blue* shift with respect to the related optical excitations of $\text{Co}(\text{CO})_4$. However, one does feel reasonably secure in associating the weaker feature around 370 nm with species IV, red-shifted with respect to the LMCT transitions of $\text{Co}(\text{CO})_4$ as well as the proposed LMCT excitation of $\text{Fe}(\text{CO})_4$, 325 nm, to be discussed later.

Vibrational Aspects. Surveying the information available from a wide variety of $\text{Co}/\text{CO}/\text{O}_2/(\text{Ar})$ matrix cocondensations, one can deduce with some confidence that besides mononuclear parent complexes $\text{Co}(\text{CO})_n$ (where $n = 1, 2, 3, 4$) one can synthesize, isolate, and identify *four* major mixed-ligand products which we chose to assign as a series of cobalt mono(dioxygen)–carbonyl complexes $\text{Co}(\text{CO})_n(\text{O}_2)$

Table III. Comparison of IR-Active $\nu(\text{CO})$ Modes for $\text{Fe}(\text{CO})_4$ and $\text{Co}(\text{CO})_4(\text{O}_2)$

| $\text{Co}(\text{CO})_4(\text{O}_2)$ $\nu(\text{CO}), \text{cm}^{-1}$ | $\text{Fe}(\text{CO})_4^a$ | | |
|--|----------------------------------|-----------------|-----------------|
| | $\nu(\text{CO}), \text{cm}^{-1}$ | I_{CO} | symmetry assign |
| 2102 | 1995 | 1.0 | A_1 |
| 2082 | 1988 | 3.3 | B_1 |
| 2076 | 1973 | 2.2 | B_2 |

^a Reference 14.

(where $n = 1, 2, 3, 4$). We realize that our conclusion regarding CO stoichiometry is not watertight because of the lack of definitive $^{12}\text{C}^{16}\text{O}/^{13}\text{C}^{16}\text{O}$ isotopic confirmation. Our stoichiometric proposals must therefore rely heavily on ligand concentration and matrix-warm-up spectral behavior, infrared $\nu(\text{CO})$ activities, spectral trends on passing from $\text{Co}(\text{CO})_n$ to the respective $\text{Co}(\text{CO})_n(\text{O}_2)$ complex, prior knowledge of the existence of a tetracarbonyl dioxygen reaction product $\text{Co}(\text{CO})_4(\text{O}_2)$ from 77 K $\text{Co}(\text{CO})_4/\text{O}_2$ condensations with ESR detection,¹³ and the chemically intuitive and reasonable expectation that each of the paramagnetic parents $\text{Co}(\text{CO})_n$ generated in the presence of O_2 has a fair opportunity of forming the corresponding $\text{Co}(\text{CO})_n(\text{O}_2)$ adduct.²¹

A number of other spectral observations can be considered to lend credence to our proposals. First, the central cobalt atom in each of the $\text{Co}(\text{CO})_n(\text{O}_2)$ complexes can be assumed to be electron deficient relative to the respective $\text{Co}(\text{CO})_n$ parent compound, in light of the anionic (electron-rich) nature of the dioxygen moiety (formulated to be between superoxo and peroxy in charge-transfer character, based on $\nu(\text{OO})$ frequencies²² lying in the range 1130 to 900 cm^{-1}). In accordance with this proposal is the recognition of *blue-shifted* $\nu(\text{CO})$ modes of $\text{Co}(\text{CO})_n(\text{O}_2)$ relative to the corresponding $\text{Co}(\text{CO})_n$ parent. In particular, the near superoxo character (1124 cm^{-1}) for the dioxygen moiety in $\text{Co}(\text{CO})_4(\text{O}_2)$ (the $\nu(\text{OO})$ mode of superoxide in alkali halide crystals occurs at 1097 cm^{-1}) concurs with the ESR bonding description for the purported same molecule.¹³ Furthermore, if a $[\text{Co}(\text{CO})_4]^+\text{O}_2^-$ molecular ion pair description is justified, the cationic tetracarbonyl fragment can be considered to be isoelectronic with $d^8 \text{Fe}(\text{CO})_4$, the latter being photolytically generated from $\text{Fe}(\text{CO})_5$ in low-temperature matrices.¹⁴ The $\text{Fe}(\text{CO})_4$ tetracarbonyl fragment has been very thoroughly characterized both theoretically²³ and experimentally (matrix IR isotopic frequency/intensity analysis, UV–visible and MCD),¹⁴ *all techniques* supporting the idea of a distorted tetrahedral molecule in which it is considered that the orbitally degenerate 3T_1 electronic ground state of the T_d molecule suffers a substantial Jahn–Teller distortion, yielding a C_{2v} (120 and 145°), high-spin structure.^{14,23}

From an infrared comparative point of view the IR-active $\nu(\text{CO})$ modes of $\text{Fe}(\text{CO})_4$ might be expected to bear a close resemblance to those of our proposed $d^8 [\text{Co}(\text{CO})_4]^+$ cation, taking into account a sizeable upward frequency shift of $[\text{Co}(\text{CO})_4]^+$ because of pronounced valence orbital stabilization effects compared to $\text{Fe}(\text{CO})_4$. As can be seen from Table III, this spectral expectation is indeed realized in practice. However, the actual orientational disposition of the superoxo moiety relative to the $[\text{Co}(\text{CO})_4]^+$ framework cannot be established from the available data, although we note that Symons et al.¹³ favor a pseudo- C_{3v} structure for $\text{Co}(\text{CO})_4(\text{O}_2)$ with an end-on type of axial superoxide coordination, while Turner et al. favor C_{2v} for $\text{Fe}(\text{CO})_4(\text{CH}_4)$ and C_{3v} for $\text{Fe}(\text{CO})_4(\text{N}_2)$.¹⁴

Significantly, the $\nu(\text{OO})$ stretching frequencies of $\text{Co}(\text{CO})_n(\text{O}_2)$ (where $n = 1, 2, 3$) tend to cluster around 940–970 cm^{-1} , in the region of $\text{Co}(\text{O}_2)$ itself (954 cm^{-1}), possibly indicative of a side-on mode of dioxygen coordination (similar

Table IV. Optical Spectra for Cobalt Atom-Carbon Monoxide-Dioxygen Matrix Cocondensation Reactions

| CO/O ₂ ≈ 1/4 | | CO/O ₂ ≈ 1/1 | | CO/O ₂ ≈ 4/1 | | species, assign |
|-------------------------|----------------------|-------------------------|----------------------|-------------------------|----------------------|---|
| 10-12 K ^b | 30-40 K ^c | 10-12 K ^b | 30-40 K ^c | 10-12 K ^b | 30-40 K ^c | |
| | 370 | | 367 | | 368 | Co(CO) ₄ (O ₂), LMCT |
| 358 | | 356 | | 356 | | Co(CO) ₄ , LMCT ^a |
| 350 sh | | 347 sh | | 347 sh | | Co(CO) ₄ , LMCT ^a |
| 310 | | 310 | | 311 | | Co(CO) ₄ , LMCT ^a |
| 245 | | 252 | | 257 | | Co(CO) ₄ , MLCT ^a |
| 232 | | 234 | | 234 | | Co(CO) ₄ , MLCT ^a |
| 222 | 222 br | 225 | 226 br | 225 | 228 br | Co(CO) ₄ (O ₂), MLCT; Co(CO) ₃ (O ₂), MLCT |

^a See ref 26 for a detailed discussion of the optical assignments of M(CO)₄ species where M = Ni, Pd, Pt, Co, Rh, and Ir. ^b Spectrum recorded on deposition at 10-12 K. ^c Spectrum recorded after warming to 30-40 K and recooling to 10-12 K.

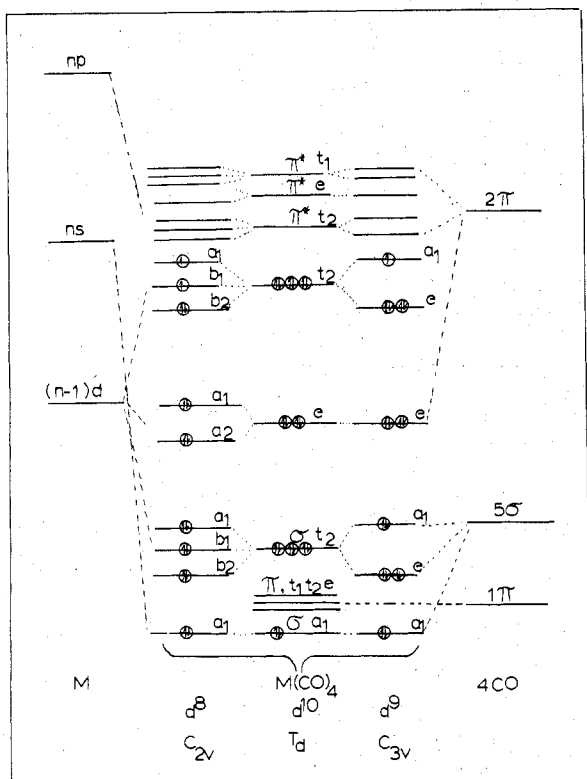
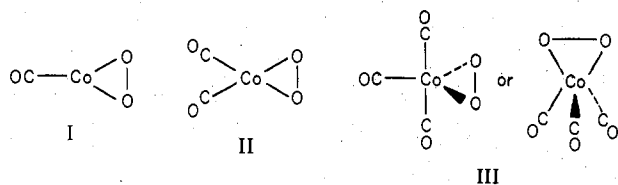


Figure 8. Qualitative energy-level scheme for T_d , C_{3v} , and C_{2v} forms of a $M(CO)_4$ moiety.^{23,26}

to 966 cm^{-1} proposed for $\text{Ni}(\text{O}_2)^{17}$ rather than end-on superoxo-like, as preferred for $\text{Co}(\text{CO})_4(\text{O}_2)$. Tentative structures for the lower stoichiometry complexes can therefore be envisaged as structures I-III which are consistent with (but



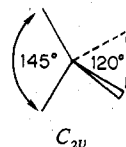
not proven by) the available infrared data. Unequivocal structural characterization of the products of the Co/CO/O₂ matrix cocondensation will have to await the results of other kinds of experiments.

Electronic Aspects. To understand the structural preferences of binary carbonyls one needs to examine the results of molecular orbital calculations. Several ab initio calculations now exist for four-, five-, and six-coordinate species,²⁴ but only two sets of calculations have focussed on a comprehensive selection of coordination numbers and d-orbital configurations.²³ The latter are both of the extended Hückel type, differing only in their parameterization, although through some

quirk in the semiempirical method slight differences in the predicted lowest energy geometries are to be found.²³

For the d^9 four-coordinate system, both sets of calculations favor the D_{2d} structure very slightly over the C_{3v} geometry. IR^{2,25} and ESR² data for $\text{Co}(\text{CO})_4$ in Ar point to a C_{3v} geometry although ESR data² demonstrate that $\text{Co}(\text{CO})_4$ can adopt a D_{2d} geometry in some matrix environments, illustrating the delicate energetic balance between the two forms. The slight distortion of $\text{Co}(\text{CO})_4$ from the regular tetrahedral geometry and the d^9 open-shell nature of the molecule are manifested in the optical spectrum²⁶ by (i) the splitting of the intense ultraviolet (250-260 nm) $\text{Co}(d) \rightarrow \text{CO}(\pi^*)$ MLCT bands, (ii) the appearance of LMCT transitions in the 300-360-nm region of the spectrum arising from electronic excitations out of low-lying ligand-metal σ -bonding combinations into the hole states that exist in the split metal t_2 (d) levels, and (iii) splitting of the LMCT absorptions themselves (see Figure 5A and Table IV).

The high-spin d^8 four-coordinate binary carbonyl system has been examined by similar molecular orbital methods²³ and is predicted to be a distorted tetrahedral (triplet) C_{2v} fragment. On the other hand, the low-spin (singlet) form is expected to be square planar.²³ Such geometries should be easily distinguished by IR and MCD matrix spectroscopy. As the semiempirical molecular orbital methods include only orbital energy terms, it is not possible to discuss the relative energies of singlet and triplet structures. Experimentally, however, IR and MCD data for $\text{Fe}(\text{CO})_4^{14}$ strongly support the C_{2v} triplet formulation with the geometry shown.



(Of note here are the calculations for C_{3v} $\text{Fe}(\text{CO})_4$, which is found to be only slightly higher in energy than the C_{2v} ground-state structure.²³) The calculated energy-level scheme for such a geometry as derived by Burdett is shown in Figure 8, together with the level orderings, symmetry designations, and correlations for T_d d^{10} $M(\text{CO})_4$, C_{2v} d^9 $M(\text{CO})_4$, and C_{2v} d^8 $M(\text{CO})_4$ tetracarbonyl moieties. Note that all d-d transitions of $\text{Fe}(\text{CO})_4$ are predicted^{14,23a} to fall in the near- to far-IR. This proposal is in accord with recent optical studies of $M(\text{CO})_4$ (where $M = \text{Ni}, \text{Pd}, \text{Pt}$)²⁶ and photoelectron measurements²⁷ for $\text{Ni}(\text{CO})_4$ which place the e to t_2 ligand field splitting energy around 5000-6000 cm^{-1} . With this information at hand we can now rationalize our optical spectroscopic observations for $\text{Co}(\text{CO})_4(\text{O}_2)$ in terms of a molecular ion-pair description, $[\text{Co}(\text{CO})_4]^+ \text{O}_2^-$, in which the d^8 cation is considered to be isostructural with its d^8 neighbor $\text{Fe}(\text{CO})_4$.

To a first approximation one can analyze the optical spectra of $\text{Fe}(\text{CO})_4$ and $[\text{Co}(\text{CO})_4]^+$ on the basis of a pseudotetrahedral d^2 hole model, in a manner not unlike that employed

Table V. Ligand-to-Metal Charge-Transfer Assignments for $\text{Co}(\text{CO})_4$, $[\text{Co}(\text{CO})_4]^+$, and $\text{Fe}(\text{CO})_4$ ^a

| $\text{Co}(\text{CO})_4$ ^b | $[\text{Co}(\text{CO})_4]^+$ ^c | $\text{Fe}(\text{CO})_4$ ^d |
|---------------------------------------|---|---------------------------------------|
| 310 | | |
| 347 sh | | 325 |
| 357 | | |
| | 370-367 | |

^a Units in nm. ^b Reference 26. ^c This study. ^d Reference 14.

to treat the d¹ hole case exemplified by $\text{Co}(\text{CO})_4$.²⁶ Optical splitting effects arising from the reduced symmetry of these molecules below that of T_d to C_{3v} or C_{2v} can be considered as a small perturbation on the optical spectra at this level of analysis (Figure 8). With this premise, certain features of the optical spectra of $\text{Co}(\text{CO})_4(\text{O}_2)$ become most significant and supportive of the ion-pair proposal. To begin, an assignment of the intense ultraviolet bands of $[\text{Co}(\text{CO})_4]^+$ to $\text{Co}(\text{d}) \rightarrow \text{CO}(\pi^*)$ MLCT transitions, *blue-shifted* with respect to the similar bands of $\text{Co}(\text{CO})_4$ (Table IV, Figures 5-7), is consistent with the idea of a higher effective nuclear charge on the cobalt atom in $\text{Co}(\text{CO})_4(\text{O}_2)$, stabilization of cobalt valence d orbitals, and an argument in favor of $[\text{Co}(\text{CO})_4]^+\text{O}_2^-$. In line with this proposal is the association of the weak absorption at 370 nm of $[\text{Co}(\text{CO})_4]^+$ with a $\text{CO}(\sigma) \rightarrow \text{Co}(\text{d})$ LMCT excitation, *red-shifted* with respect to the similar LMCT transitions observed at 310-358 nm for $\text{Co}(\text{CO})_4$ and at 325 nm for $\text{Fe}(\text{CO})_4$ (Table V). One must assume in this discussion that superoxide intraligand $\pi \rightarrow \pi^*$ transitions and/or $\text{O}_2(\pi) \rightarrow \text{Co}(\text{d})$ LMCT transitions, also anticipated in the 200-300-nm region, either are overlapped and hidden by the intense $\text{Co}(\text{d}) \rightarrow \text{CO}(\pi^*)$ MLCT bands or are too weak to observe in our spectra.

Acknowledgment. The generous financial assistances of the National Research Council of Canada's New Ideas, Strategic Energy, and Operating Grant Programmes, the Atkinson Foundation, the Connaught Fund, Imperial Oil of Canada, the Lash Miller Chemical Laboratories, and Erindale College are all gratefully appreciated. A.J.L.H. and W.J.P. gratefully acknowledge the NRCC for scholarships throughout the period of their graduate research.

Registry No. I, 70713-65-4; II, 70713-66-5; III, 70775-25-6; IV, 52633-53-1; $[\text{Co}(\text{CO})_4]^+$, 70002-18-5.

References and Notes

- G. A. Ozin and A. J. Lee Hanlan, *Inorg. Chem.*, in press; G. A. Ozin in "Vibrations in Adsorbed Layers", Kernforschungsanlage (KFA), Jülich, West Germany, 1978.
- E. P. Kündig, A. J. Lee Hanlan, H. Huber, B. R. McGarvey, and G. A. Ozin, *J. Am. Chem. Soc.*, **97**, 7054 (1975).
- G. A. Ozin and A. Vander Voet, unpublished work.
- A. J. Lee Hanlan, H. Huber, and G. A. Ozin, to be submitted for publication.
- A. J. Lee Hanlan and G. A. Ozin, *Inorg. Chem.*, **16**, 2848, 2857 (1977).
- A. J. Lee Hanlan, G. A. Ozin, and W. J. Power, *Inorg. Chem.*, **17**, 3648 (1978).
- See for example M. McGlinchey and P. Skell in "Cryochemistry", M. Moskovits and G. A. Ozin, Eds., Wiley, New York, 1976, Chapter 5.
- H. Huber and G. A. Ozin, *Inorg. Chem.*, **16**, 64 (1977).
- D. McIntosh, H. Huber, and G. A. Ozin, *Inorg. Chem.*, **16**, 975 (1977).
- G. A. Ozin, *Acc. Chem. Res.*, **10**, 21 (1977).
- E. P. Kündig, M. Moskovits, and G. A. Ozin, *Can. J. Chem.*, **51**, 2737 (1973).
- W. Klotzbücher and G. A. Ozin, *J. Am. Chem. Soc.*, **97**, 3965 (1975).
- S. A. Fieldhouse, B. W. Fullam, G. W. Neilson, and M. C. R. Symons, *J. Chem. Soc., Dalton Trans.*, 567 (1974).
- (a) M. Poliakoff and J. J. Turner, *J. Chem. Soc., Dalton Trans.*, 1351 (1973); 2276 (1974); (b) A. McNeish, M. Poliakoff, K. P. Smith, and J. J. Turner, *J. Chem. Soc., Chem. Commun.*, 859 (1976); (c) T. J. Barton, R. Grinter, A. J. Thompson, B. Davies, and M. Poliakoff, *ibid.*, 841 (1978); (d) J. K. Burdett, *J. Chem. Soc., Faraday Trans. 2*, **70**, 1599 (1975); (e) M. Elian and R. Hoffmann, *Inorg. Chem.*, **14**, 1058, 1975; (f) B. Davies, A. McNeish, M. Poliakoff, M. Tranquille, and J. J. Turner, *J. Chem. Soc., Chem. Commun.*, 36 (1978); (g) T. J. Barton, I. N. Douglas, R. Grinter, and A. J. Thompson, *Ber. Bunsenges. Phys. Chem.*, **80**, 202 (1976).
- E. P. Kündig, M. Moskovits, and G. A. Ozin, *J. Mol. Struct.*, **14**, 137 (1972).
- M. Moskovits and G. A. Ozin, *Appl. Spectrosc. (Engl. Transl.)*, **26**, 481 (1972).
- H. Huber, W. Klotzbücher, G. A. Ozin, and A. Vander Voet, *Can. J. Chem.*, **51**, 2755 (1973).
- (a) J. H. Darling, M. B. Garton Sprenger, and S. J. Ogden, *Faraday Symp. Chem. Soc., No. 8*, 75 (1974); (b) D. McIntosh and G. A. Ozin, unpublished work.
- Small matrix concentration-dependent shifts are observed for the $\nu(\text{OO})$ stretching modes.
- A. J. Lee Hanlan and G. A. Ozin, *J. Am. Chem. Soc.*, **96**, 6324 (1974).
- In preliminary experiments aimed at an independent synthesis and IR characterization of the proposed Symons et al.¹³ compound $\text{Co}(\text{CO})_4(\text{O}_2)$ by the route of Knudsen cell evaporation of $\text{Co}_2(\text{CO})_8$ and simultaneous cocondensation with O_2 , we found that the actual concentration of $\text{Co}(\text{CO})_4$ that could be matrix trapped in Ar at 10-12 K from thermolyzed $\text{Co}_2(\text{CO})_8$ was extremely small as seen through the relatively "insensitive eye" of the IR probe; however, it seems that with the "supersensitive eye" of the ESR monitor, there is no difficulty at all in detecting minute amounts of either $\text{Co}(\text{CO})_4$ or its reaction product with O_2 , namely, $\text{Co}(\text{CO})_4(\text{O}_2)$ (Kündig and Ozin, unpublished work).
- A. B. P. Lever and H. B. Gray, *Acc. Chem. Res.*, **11**, 348 (1978), and references therein.
- (a) J. K. Burdett, *J. Chem. Soc., Faraday Trans. 2*, **70**, 1599 (1974); (b) M. Elian and R. Hoffmann *Inorg. Chem.*, **14**, 1058 (1975).
- (a) J. Demuyneck, A. Strich, and A. Veillard, *Nouv. J. Chim.*, **1**, 217 (1977); (b) P. J. Hay, *J. Am. Chem. Soc.*, **100**, 2411 (1978); (c) I. H. Hillier and V. R. Saunders, *Chem. Commun.*, 642 (1971); (d) R. Osman, C. S. Ewig, and J. R. Van Wazer, *Chem. Phys. Lett.*, **39**, 27 (1976); **54**, 392 (1978).
- O. Crichton, M. Poliakoff, A. J. Rest, and J. J. Turner, *J. Chem. Soc., Dalton Trans.*, 1321 (1973).
- A. B. P. Lever, G. A. Ozin, A. J. L. Hanlan, W. J. Power, and H. B. Gray, *Inorg. Chem.*, in press.
- (a) I. H. Hillier, M. F. Guest, B. R. Higginson, and D. R. Lloyd, *Mol. Phys.*, **27**, 215 (1974); (b) J. Demuyneck, *Chem. Phys. Lett.*, **45**, 74 (1977); (c) J. Demuyneck and A. Veillard, *Theor. Chim. Acta*, **28**, 241 (1973); (d) D. R. Lloyd and E. W. Schlag, *Inorg. Chem.*, **8**, 2544 (1969).